JOURNAL OF MATERIALS SCIENCE **35** (2000) 1253–1256

Comparative investigation of the nitrogenation mechanisms of bulk intermetallic $Sm_2(Fe,Co)_{17}$ by two processes

D. LEMARCHAND*, V. DE PAUW
UMR CNRS 6634, Groupe de Métallurgie Physique, Faculté des Sciences et Techniques, Université de Rouen, 76821 Mont-Saint-Aignan Cedex, France
E-mail: dany.lemarchand@univ-rouen.fr

The nitrogenation mechanisms of the $Sm_2(Fe_{0.5}Co_{0.5})_{17}$ compound were investigated on bulk samples using X-ray diffraction and chemical analysis. Two nitrogenation processes (fluidized bed nitrogenation (FBN) and gaseous nitrogenation (GN)) were used in order to compare the different steps occurring during the treatment. The fluidized bed process leads to a constant nitrogen surface concentration after one hour treatment while the concentration increases continuously with the gaseous process. The overall bulk nitrogenation kinetics is parabolic for the fluidized bed, whereas the gaseous nitrogenation exhibits first an incubation period followed by an accelerated rate. Two different mechanisms, bulk diffusion for the FBN process and an interface reaction for the GN process, govern the nitrogenation kinetics. *© 2000 Kluwer Academic Publishers*

1. Introduction

Since the discovery of the $Sm_2Fe_{17}N_y$ ($y \leq 4$) nitride, which exhibits very promising magnetic properties, by Coey and Sun in 1990 [1, 2], several studies were devoted to understanding the nitrogenation mechanisms of Sm_2Fe_{17} powders, in relation to the nitrogenation process used [3–5].

In a previous work [6], we investigated the influence of the nitriding process on the nitrogen distribution in the bulk compound $Sm_2(Fe,Co)_{17}$. In addition to the usual gaseous process, a fluidized bed was also used. This study has shown that both processes involved different nitrogenation mechanisms. The cross-sectional investigation of the nitrided samples revealed that, with the fluidized bed process, the nitrogen distribution forms a nitrided layer parallel to the surface whereas, with the gaseous nitrogenation, nitrogen first diffuses along microcracks present in the samples [6, 7].

In the present work, both nitrogenation kinetics of the surface layer and the overall nitrogenation kinetics of the alloy are investigated in order to get a better understanding of the mechanisms involved in these processes.

2. Experimental

We investigated a commercial as-cast alloy (from Johnson-Matthey), whose composition is close to the $Sm_2(Fe_{0.5}Co_{0.5})_{17}$ stoichiometry. Cobalt addition to the Sm_2Fe_{17} compound aimed at improving its intrinsic magnetic properties. The microstructure of this alloy is made up of three phases [7, 8]: the matrix $Sm_2(Fe_{0.5}Co_{0.5})_{17}$ (79 vol. % of the alloy), a dendritic phase ($Fe_{0.6}Co_{0.4}$) with the bcc α-Fe lattice (14 vol. %), and $Sm(Fe_{0.6}Co_{0.4})_3$ (7 vol. %).

The samples were cut into 2 mm thick platelets. Two different nitrogenating processes were then applied to the samples:

– An usual gaseous nitrogenation (GN) process, i.e. a heat treatment in a gas flow.
– A fluidized bed nitrogenation (FBN) process. Details on this process are given in Refs. [6, 7].

The nitrogenating gas in both processes was a mixture of $N_2 + NH_3$ (60/40 vol. %) with a rate of gas flow of 0.7 m^3N/h.

The nitrided flat surfaces of the platelet-like samples were investigated by reflection X-ray diffraction (XRD) using Co K_α radiation. The analyzed depth by this technique (i.e. the thickness from which comes 95% of the diffracted X-ray intensity) is about 3 μm for an incidence angle of 8°.

Due to the overlap of the X-ray emission lines L_{α^1} Co (second order) and K_{α^1} N (first order), the nitrogen surface concentration cannot be determined by using electron probe microanalysis. Katter *et al.* and Wei *et al.* [9, 10] have reported an expansion of the Sm_2Fe_{17} lattice, dependent on the nitrogen content, which suggested the existence of intermediate R_2Fe_{17}-nitrides. Such an expansion was observed in our nitrided samples, and the lattice parameters of the

---

[*] Author to whom all correspondence should be addressed.

$Sm_2(Fe_{0.5}Co_{0.5})_{17}N_y$ phase were determined from the reflection XRD spectra. The nitrogen surface concentration c_s was therefore estimated for the samples from the known dependence of the lattice parameters on the nitrogen content [9, 10].

The nitrided platelets were ground and their nitrogen content determined by chemical analysis, as explained in Ref. [6]. From the mass and the surface of the platelets, this analysis allowed us to determine the amount $M(t)$ of nitrogen introduced per surface unit of the samples during each treatment.

3. Results

3.1. Nitrogenation kinetics of the surface layer

The nitrogen surface concentration c_s dependence on the nitrogenation time is shown in Figs 1 and 2, respectively for the FBN and GN processes. It can be seen that the c_s variation is different for the two processes.

With the FBN process (Fig. 1), the isothermal curves exhibit the same behaviour. After one hour treatment, c_s reaches a constant value and a saturation plateau is achieved rapidly. These plateaux increase in relation to the temperature.

With the GN process (Fig. 2), c_s increases continuously with the nitrogenation time. No saturation plateau is obtained, except for the curve at 560°C which shows a plateau close to $y = 3.5$ after 4 h treatment. This value is close to the maximum nitrogen content in $Sm_2Fe_{17}N_y$ ($y = 4$) reported in the literature [5, 10].

This study by XRD confirms that different mechanisms occur in both nitrogenation processes. The different nitrogen distribution according to the process, reported in a previous paper [6], can be correlated with differences in the nitrogenation kinetics of the surface layer.

3.2. Overall nitrogenation kinetics of the alloy

The amount of nitrogen introduced in the platelet samples per surface unit $M(t)$ is calculated from the quantitative chemical analysis data. Figs 3 and 4 show the $M(t)$ plot as a function of time for each nitrogenation process. These kinetics again show a difference of behaviour for both processes.

3.2.1. FBN process

With the FBN process (Fig. 3), the $M(t)$ dependence on the square root of time can be expressed as: $M(t) = k\,t^{1/2}$ (parabolic rate law), where k depends on the temperature. Such a behaviour indicates that the nitrogenation kinetics is controlled by the nitrogen diffusion in the sample. Taking into account that the surface concentration c_s is constant during the treatment (Fig. 1), the solution of Fick's equations indicates that the k coefficient may be written, for each temperature [11]:

$$k = 2c_s\sqrt{\frac{D}{\pi}} \tag{1}$$

where D is the nitrogen diffusion coefficient at the temperature T. The diffusion coefficients obtained from Equation 1 are reported in Table I and will be discussed later.

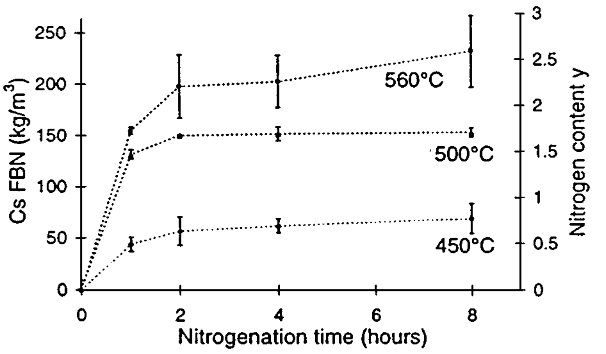

Figure 1 Dependence of the nitrogen surface concentration c_s on the nitrogenation time with the FBN process.

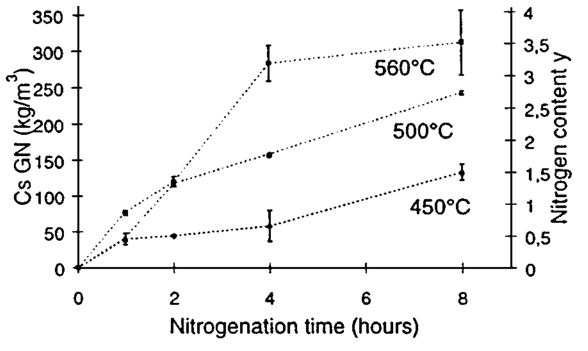

Figure 2 Dependence of the nitrogen surface concentration c_s on the nitrogenation time with the GN process.

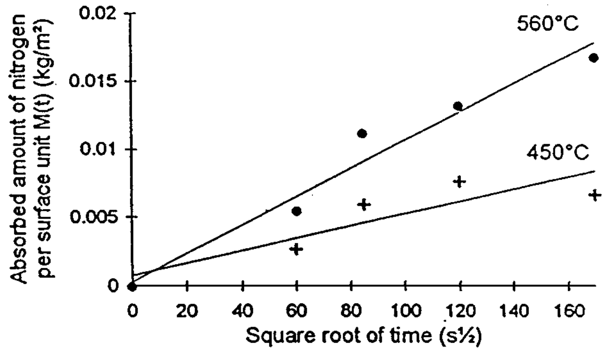

Figure 3 Dependence of the absorbed amount of nitrogen per surface unit $M(t)$ on the square root of nitrogenation time with the FBN process.

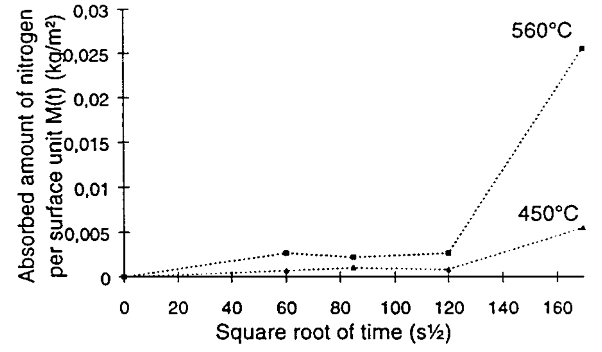

Figure 4 Dependence of the absorbed amount of nitrogen per surface unit $M(t)$ on the square root of nitrogenation time with the GN process.

TABLE I Nitrogen diffusion coefficients in $Sm_2(Fe_{0.5}Co_{0.5})_{17}$ at different temperatures for the FBN process

Temperature	D_{FBN} ($mm^2 \cdot s^{-1}$)
450°C	3.3×10^{-7}
560°C	1.6×10^{-7}

3.2.2. GN process

The kinetics is more complex with the GN process (Fig. 4) than with the FBN process. The kinetics first exhibits an incubation period (more than 4 hours) while $M(t)$ increases very slowly, then the rate is accelerated with time. As shown in Fig. 2, c_s increases continuously during this incubation. It is inferred that the bulk diffusion process is activated only when c_s exceeds a critical threshold. This can be determined from Fig. 2 to be roughly similar to the value reached at the plateau for the FBN process (Fig. 1). After the incubation, c_s continue to increase, thus explaining the accelerated rate for the overall nitrogenation kinetics.

3.2.3. Nitrogen diffusion coefficients

The nitrogen bulk diffusion coefficients D in $Sm_2(Fe_{0.5}Co_{0.5})_{17}$ for the FBN process are reported in Table I. Contrary to the expected behaviour, the diffusion coefficient decreases with increasing temperature. That means that an atomic process affecting the $Sm_2(Fe_{0.5}Co_{0.5})_{17}$ lattice couterbalances the thermal activation of the diffusion process. Though the origin of this atomic process is not yet clear, several assumptions can be made:

i) $Sm_2(Fe_{0.5}Co_{0.5})_{17}$ is known to be somewhat unstable at high temperature and can slowly disproportionate into the nitrides SmN and Fe_4N [12]. These precipitates could act as a diffusion barrier and decrease the apparent diffusion coefficient through the matrix at higher temperatures. Since lattice disproportionation is facilitated by mechanical stress due to the nitriding expansion [12], and since such stresses are easier to release in a single isolated particle than in the bulk, this effect is expected to be more important in bulk material than in powders.

ii) dissociation of the gaseous atmosphere of ammonia into hydrogen and nitrogen during the treatment leads to the introduction of hydrogen into the matrix, and this is associated with an expansion of the $Sm_2(Fe_{0.5}Co_{0.5})_{17}$ lattice. This expansion distends the Fe-Fe atomic distance and could facilitate nitrogen diffusion. The amount of hydrogen in the lattice decreases as the temperature increases [12]; this could lead to less enhancement for the high temperature nitrogen diffusion coefficient.

Data on nitrogen diffusion in Sm_2Fe_{17}, obtained by several groups [3, 4, 13–17] are plotted on the Arrhenius diagram displayed in Fig. 5. They are compared to the values reported in Table I. It can be seen that our experimental curves are above those drawn from the different published data. The latter data are obtained over a wide range of experimental conditions: process, gaseous atmosphere and grain size of the powder. The D values obtained in this study are closer to the data obtained in similar experimental condition, i.e. with a gaseous atmosphere of ammonia [13] and with bulk samples [14]. Contrary to expectation, it seems that the use of a pure nitrogen atmosphere, or of a reduced grain size, decreases the diffusion coefficient [3, 4, 15–17].

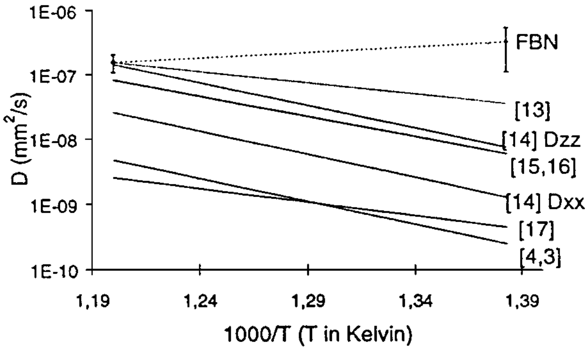

Figure 5 Arrhenius plots for the diffusion coefficients from different groups and from this study.

4. Discussion

4.1. The different stages of the nitrogenation mechanism

The overall mechanism leading to the nitrogenation of the bulk compound $Sm_2(Fe,Co)_{17}$ from the nitriding gas can be described by three different stages in both processes:

(1) Transport of reactive molecules (N_2 or NH_3) of gas from the fluid phase to the bulk surface.

(2) Adsorption of these reactive molecules at the bulk surface, and dissociation of these molecules leading to the formation of atomic nitrogen N.

(3) Diffusion of N atoms in the bulk to form the nitride $Sm_2(Fe,Co)_{17}N_y$.

4.2. Stage controlling the overall nitrogenation kinetics

Stage (1), which is a mass transport (by diffusion or convection) in a fluid, will always be more rapid than stage (3) (transport by diffusion in the solid). So the former cannot control the overall kinetics in both processes.

With the FBN process, the overall nitrogenation kinetics follows a parabolic rate law, which indicates that stage (3) controls the kinetics. The surface concentration c_s reaches rapidly a saturation plateau c_{s0}, so c_s can be considered as constant for each temperature.

With the GN process, the overall kinetics exhibits an incubation during which the surface concentration c_s increases progressively to a critical threshold; then the kinetics is accerated with time. Such a behaviour indicates that the overall nitrogenation kinetics is controlled by an interfacial reaction, made up of the stage (2), i.e. the N_2 and NH_3 adsorption/dissociation stage.

The rapid achievement of a saturation plateau with the FBN process, and the related absence of the incubation period, can be attributed to two effects due to the fluidized bed particles impacts at the sample surface:

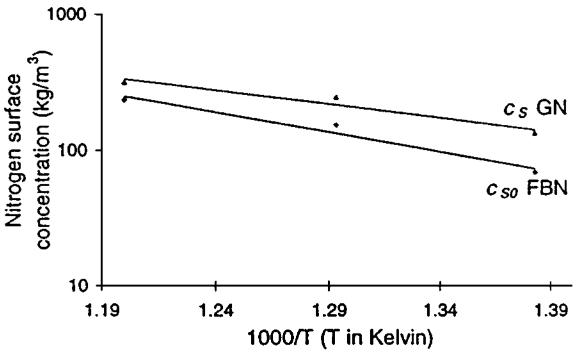

Figure 6 Arrhenius plots for the c_{s0} and $c_{s(\max)}$ values obtained with the two nitrogenation processes.

(1) On the one hand, the momentum transfer during the particles/sample surface collision activates the adsorption and/or the dissociation of N_2 molecules, leading to an enhanced kinetics of the interfacial reaction with the FBN process.

(2) On the other hand, the fluidized bed particles impacts increase the surface roughness, contributing also to the acceleration of the interfacial reaction [7, 8].

4.3. Comparison of the c_s maximum values for both processes

The Arrhenius plot for the surface concentration c_{s0} obtained from the plateau values with the FBN process is reported in Fig. 6. Although they do not correspond to an equilibrium plateau, the c_s values achieved for 8 h treatment with the GN process are also displayed in Fig. 6 to compare the two nitrogenation processes.

The fact that the c_{s0} plateau value with the FBN process is smaller than the c_s maximum value with the GN process, seems to result from an equilibrium between the adsorption and the desorption of nitrogen molecules under the influence of the particles impacts. Though the momentum transfer favours the molecules adsorption at the surface, it is assumed that above a surface concentration limit, the reverse process i.e. molecule desorption due to the particles impacts can occur competitively. It results an equilibrium concentration corresponding to the c_{s0} plateau value.

The Arrhenius plots for both processses in Fig. 6 shows that straight lines are obtained in the studied temperature range. For the FBN process, the activation energy, deduced from the slope, is $E_a = 55 \pm 20\,\mathrm{kJ{\cdot}mol^{-1}}$. This behaviour indicates that the competition between adsorption and desorption at the sample surface is a thermally activated process. The physical meaning of the Arrhenius straight line is less clear for the GN process, as it does not correspond to equilibrium plateau values for the $c_s(t)$ curves (Fig. 2).

5. Conclusion

Most previous studies on the nitrogenation of Sm_2Fe_{17}-type compounds were devoted to powdered samples. In this work, the investigation of $Sm_2(Fe_{0.5}Co_{0.5})_{17}$ samples in the bulk form, allowed us to reveal different nitrogenation mechanisms in relation to two different nitrogenation processes (FBN and GN).

The FBN process leads, in less than an hour, to a constant nitrogen surface concentration. Nitrogen diffusion takes place from this surface and governs the overall kinetics, which results to be parabolic. This leads to a homogeneous nitrogenated layer at the surface of the bulk sample [6].

At the opposite, the GN process leads to a continuously increasing surface concentration. After an incubation period, the overall kinetics becomes accelerated. This behaviour is consistent with an interfacial reaction-controlled nitrogenation mechanism. The resulting nitrogenated layer becomes irregular and much more diffuse than with the FBN process [6].

The existence of such bulk mechanisms could be of importance in the fundamental understanding of nitrogenation of powders.

References

1. J. M. D. COEY and H. SUN, *J. Magn. Magn. Mater.* **87** (1990) L251.
2. H. SUN, J. M. D. COEY, Y. OTANI and D. P. F. HURLEY, *J. Phys.: Condens. Matter* **2** (1990) 6465.
3. J. M. D. COEY, R. SKOMSKI and S. WIRTH, *IEEE Trans. Magn.* **28** (1992) 2232.
4. R. SKOMSKI and J. M. D. COEY, *J. Appl. Phys.* **73**(11) (1993) 7602.
5. S. BRENNAN, R. SKOMSKI and J. M. D. COEY, *IEEE Trans. Magn.* **30** (1994) 571.
6. V. DE PAUW, D. LEMARCHAND and C. IACOB, *J. Alloys Compd.* **265** (1998) 286.
7. V. DE PAUW, thesis, University of Rouen, France, 1996.
8. V. DE PAUW, D. LEMARCHAND and A. FNIDIKI, *J. Magn. Magn. Mater.* **169** (1997) 82.
9. M. KATTER, J. WECKER, C. KUHRT, L. SCHULTZ and R. GRÖSSINGER, *ibid.* **114** (1992) 35.
10. Y. N. WEI, K. SUN, Y. B. FEN, J.-X. ZHANG, B. P. HU, Y.-Z. WANG, X.-L. RAO and G.-C. LIU, *J. Alloys Compd.* **194** (1993) 9.
11. J. PHILIBERT, "Atoms Movements: Diffusion and Mass Transport in Solids" (Les Editions de Physique, Les Ulis, 1991) p. 1.
12. R. SKOMSKI, S. BRENNAN and S. WIRTH, "Interstitial Intermetallic Alloys, NATO ASI Series, Serie E: Applied Sciences," Vol. 281, edited by F. Grandjean, G. J. Long and K. H. J. Buschow (Kluwer Academic Publishers 1995) p. 371.
13. H. KANEKO, T. KURINO and H. UCHIDA, in Proc. 7th Int. Symp. on Magnetic Anisotropy and Coercivity in RE-TM Alloys Canberra, Australia, 1992, p. 320.
14. C. N. CHRISTODOULOU and N. KOMADA, *J. Alloys Compd.* **222** (1995) 27.
15. H. UCHIDA, S. TACHIBANA, T. KAWANABE, Y. MATSUMURA, V. KOENINGER, H. H. UCHIDA, H. KANEKO and T. KURINO, *ibid.* **222** (1995) 107.
16. U. KOIKE, K. KAMADA, H. UCHIDA, V. KOENINGER, Y. MATSUMURA, H. H. UCHIDA, T. KURINO and H. KANEKO, in Proc. 12th Int. Workshop on RE Magnets and Their Applications Canberra, Australia, 1992, p. 237.
17. J. M. D. COEY, J. F. LAWLER, H. SUN and J. E. M. ALLAN, *J. Appl. Phys.* **69**(5) (1991) 3007.

Received 5 August 1998
and accepted 19 August 1999